ORNL/TM-6146

Analysis of a Neutron Scattering and Gamma-Ray Production Integral Experiment on Aluminum for Neutron Energies from 1 to 15 MeV

S. N. Cramer
E. M. Oblow

OAK RIDGE NATIONAL LABORATORY
OPERATED BY UNION CARBIDE CORPORATION · FOR THE DEPARTMENT OF ENERGY

DISCLAIMER

Printed in the United States of America. Available from
National Technical Information Service
U.S. Department of Commerce
5285 Port Royal Road, Springfield, Virginia 22161
Price: Printed Copy $4.50; Microfiche $3.00

ORNL/TM-6146

Contract No. W-7405-eng-26

Neutron Physics Division

ANALYSIS OF A NEUTRON SCATTERING AND GAMMA-RAY PRODUCTION INTEGRAL EXPERIMENT ON ALUMINUM FOR NEUTRON ENERGIES FROM 1 TO 15 MeV

S. N. Cramer and E. M. Oblow

This Work Supported by
DEFENSE NUCLEAR AGENCY
Under Subtask PE083

Date Published - January 1978

OAK RIDGE NATIONAL LABORATORY
Oak Ridge, Tennessee 37830
operated by
UNION CARBIDE CORPORATION
for the
DEPARTMENT OF ENERGY

Manuscript Typed by Ann Houston

Table of Contents

		Page No.
	Abstract	v
I.	Introduction	1
II.	Experimental Arrangements	1
III.	Calculational Model	2
	A. Codes	2
	B. Cross-Section Data and Material Specification	2
	C. Calculational Procedure	2
IV.	Comparison of Experimental and Calculated Results	7
V.	Discussion	7

THIS PAGE

WAS INTENTIONALLY

LEFT BLANK

Abstract

Monte Carlo calculations were made to analyze the results of an integral experiment with an aluminum sample to determine the adequacy of ENDF/B-IV neutron scattering and gamma-ray production cross-section data for aluminum. The experimental results analyzed included energy-dependent NE-213 detector neutron and gamma-ray count rates at a scattering angle of 125 deg and pulse-height spectra for scattered neutrons and gamma-rays. The experiments were carried out with the ORELA 1- to 20-MeV pulsed neutron source. The pulse-height data were unfolded to generate secondary neutron and gamma-ray spectra at 125 deg as a function of incident neutron energy. Multigroup Monte Carlo calculations using the MORSE code and ENDF/B-IV cross sections were made to analyze all reported results. Discrepancies between calculated and measured responses were found for secondary neutron scattering data above 10 MeV and for gamma-rays produced at energies between 4 and 7 MeV. A detailed analysis has not yet been performed to determine the reasons for these discrepancies.

THIS PAGE

WAS INTENTIONALLY

LEFT BLANK

Acknowledgement

The authors wish to acknowledge the aid of J. D. Drischler in preparing the graphical results. The multigroup cross sections were generated by W. E. Ford as part of the AMPX project of the Computer Sciences Division.

I. Introduction

Calculations of neutron and gamma-ray integral count rates and secondary energy spectra have been performed for comparison with integral experiments on aluminum. These calculations and the experiments, conducted at Oak Ridge National Laboratory, are part of the Defense Nuclear Agency data testing program designed to test neutron scattering and gamma-ray production data for several nuclides of interest for incident neutron energies from 1 to 15 MeV. The experimental data are reported in Ref. 1.

The calculations, experiments, and comparisons to be presented here are similar to those given in earlier reports.[2-5] In these earlier reports, the procedures for the data testing program are outlined in terms of experimental techniques, calculational models, and methods of data comparison.

The experiment consisted of an aluminum ring pulsed by a collimated beam of neutrons traveling approximately 50 meters from source to sample. An NE213 detector was used for detecting both neutrons and gamma rays and it was located on the center line of the ring creating an approximately 125-deg scattering angle with respect to the incident beam. The data were reduced to neutron and gamma-ray counts as a function of time and reported as counts per incident neutron as a function of incident neutron energy by using time-of-flight considerations. Pulse-height information was also recorded as a function of arrival time so that the differential spectrum of neutrons and gamma rays could be obtained by unfolding techniques as a function of incident neutron energy.

All calculations were made with the MORSE multigroup Monte Carlo code[6] using coupled neutron-gamma ray multigroup data processed by the AMPX code system.[7] The data set used was DNA aluminum MAT 4193 (ENDF/B-IV MAT 1193).

II. Experimental Arrangements

The Oak Ridge Electron Linear Accelerator (ORELA) was used to create a white pulsed source (12 nsec burst width) from the Be(γ,n) reaction. These neutrons were collimated into a beam and traveled 47.72 meters along a flight path to the scattering sample forming a uniformly distributed monodirectional source at the sample position.

The scattering sample consisted of an aluminum ring with a width of 2.704 g/cm^3. The sample and detector are shown schematically in Fig. 1. More specifications of the experiment can be found in Ref. 1. The 4.22 cm x 4.65 cm NE213 detector, used for both neutron and gamma-ray detection, was placed at a position corresponding to a scattering angle of 125 deg with respect to the incident direction. The experimental data consisted of integral count rates and energy spectra for both neutrons and gamma rays at the detector position.

III. Calculational Model

A. Codes

All calculations presented in this report were made with the MORSE multigroup Monte Carlo code using coupled neutron-gamma multigroup data processed by the AMPX code system.

B. Cross-Section Data and Material Specification

The scattering sample was taken as pure aluminum using DNA MAT 4193 MOD 0 with density of 0.06057 at/barn-cm.

The cross sections for each case were processed by AMPX into a 103-38 coupled neutron-gamma group structure with a P_7 Legendre expansion. The cross-section group structure is shown in Table 1. The neutron groups are equally spaced in lethargy between 20 MeV and 300 keV. The calculation was run in the MORSE primary particle mode in which gamma rays are produced utilizing neutron group to gamma group transfer probabilities and also the gamma-ray angular production data.

C. Calculational Procedure

Neutron histories in each energy group were given initial times determined by the neutron time-of-flight at the midpoint of each energy group to the leading edge of the sample. Relativistic velocities were used throughout the calculations. The initial times were smeared with a Gaussian approximation of the experimentally determined time spread as follows:

$$\Delta t = (R1 - RZ) \times T \qquad (1)$$

where R1 and R2 are random numbers and T = 12 nsec.

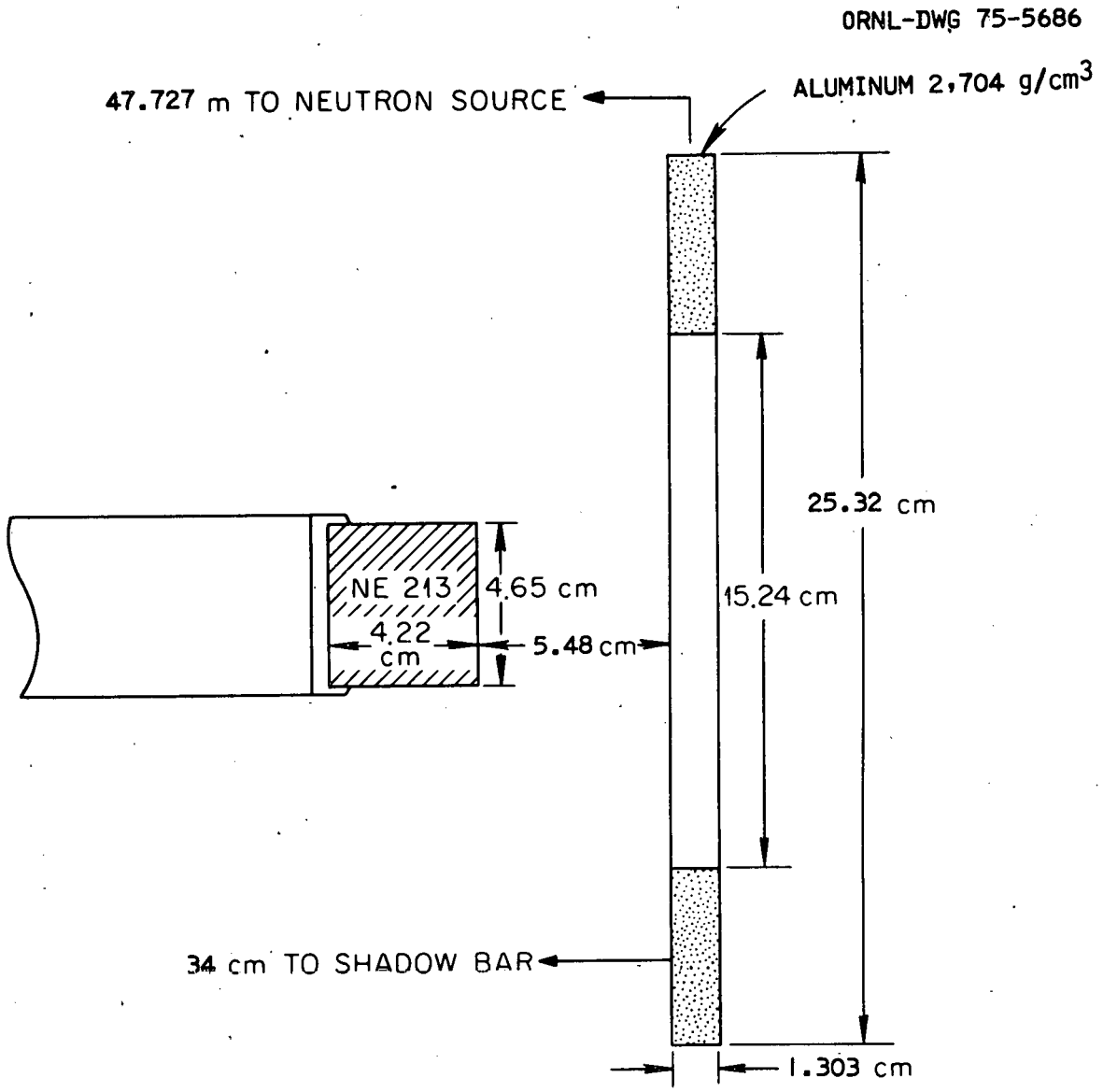

Fig. 1. Schematic Diagram of the Details of the Scattering Sample and Detector.

Table 1. Energy Group Structure and Detector Response

Group No.	Upper Energy (eV)	Detector Efficiency	Group No.	Upper Energy (eV)	Detector Efficiency
1	2.0000E 07	1.4880E-01	51	3.3652E 06	2.7240E-01
2	1.9300E 07	1.4940E-01	52	3.2474E 06	2.7570E-01
3	1.8624E 07	1.4990E-01	53	3.1337E 06	2.7880E-01
4	1.7972E 07	1.5000E-01	54	3.0239E 06	2.8180E-01
5	1.7342E 07	1.4900E-01	55	2.9180E 06	2.8470E-01
6	1.6735E 07	1.4740E-01	56	2.8159E 06	2.8750E-01
7	1.6149E 07	1.4600E-01	57	2.7173E 06	2.8980E-01
8	1.5584E 07	1.4600E-01	58	2.6621E 06	2.9250E-01
9	1.5038E 07	1.4640E-01	59	2.5303E 06	2.9570E-01
10	1.4511E 07	1.4740E-01	60	2.4417E 06	2.9830E-01
11	1.4003E 07	1.4880E-01	61	2.3562E 06	3.0080E-01
12	1.3513E 07	1.5050E-01	62	2.2737E 06	3.0320E-01
13	1.3040E 07	1.5250E-01	63	2.1941E 06	3.0520E-01
14	1.2583E 07	1.5490E-01	64	2.1172E 06	3.0710E-01
15	1.2142E 07	1.5730E-01	65	2.0431E 06	3.0900E-01
16	1.1717E 07	1.5880E-01	66	1.9715E 07	3.1070E-01
17	1.1307E 07	1.6010E-01	67	1.9025E 06	3.1240E-01
18	1.0911E 07	1.6120E-01	68	1.8359E 06	3.1390E-01
19	1.0529E 07	1.6220E-01	69	1.7716E 06	3.1540E-01
20	1.0160E 07	1.6320E-01	70	1.7096E 06	3.1680E-01
21	9.8044E 06	1.6500E-01	71	1.6497E 06	3.1810E-01
22	9.4611E 06	1.6710E-01	72	1.5919E 06	3.1850E-01
23	9.1298E 06	1.6930E-01	73	1.5362E 06	3.1860E-01
24	8.8101E 06	1.7170E-01	74	1.4833E 06	3.1840E-01
25	8.5016E 06	1.7420E-01	75	1.4305E 06	3.1810E-01
26	8.2039E 06	1.7680E-01	76	1.3804E 06	3.1760E-01
27	7.9166E 06	1.8050E-01	77	1.3321E 06	3.1700E-01
28	7.6391E 06	1.8460E-01	78	1.2854E 06	3.1630E-01
29	7.3719E 06	1.8900E-01	79	1.2404E 06	3.1540E-01
30	7.1138E 06	1.9360E-01	80	1.1970E 06	3.1230E-01
31	6.8647E 06	1.9810E-01	81	1.1551E 06	3.0750E-01
32	6.6243E 06	2.0270E-01	82	1.1146E 06	3.0220E-01
33	6.3923E 06	2.0740E-01	83	1.0756E 06	2.9640E-01
34	6.1685E 06	2.1210E-01	84	1.0379E 06	2.9030E-01
35	5.9525E 06	2.1640E-01	85	1.0016E 06	2.8380E-01
36	5.7440E 06	2.2040E-01	86	9.6649E 05	2.7700E-01
37	5.5429E 06	2.2420E-01	87	9.3265E 05	2.7000E-01
38	5.3488E 06	2.2790E-01	88	9.0000E 05	2.5180E-01
39	5.1615E 06	2.3150E-01	89	8.3644E 05	2.2080E-01
40	4.9808E 06	2.3490E-01	90	7.7737E 05	1.8670E-01
41	4.8064E 06	2.3840E-01	91	7.2247E 05	1.5040E-01
42	4.6380E 06	2.4180E-01	92	6.7145E 05	1.1260E-01
43	4.4756E 06	2.4520E-01	93	6.2403E 05	7.9640E-02
44	4.3189E 06	2.4840E-01	94	5.7996E 05	5.8360E-02
45	4.1677E 06	2.5190E-01	95	5.3900E 05	3.9970E-02
46	4.0217E 06	2.5530E-01	96	5.0093E 05	2.3900E-02
47	3.8809E 06	2.6220E-01	97	4.6555E 05	9.8650E-03
48	3.7450E 06	2.6220E-01	98	4.3268E 05	5.7930E-04
49	3.6139E 06	2.6560E-01	99	4.0212E 05	0.0
50	3.4873E 06	2.6900E-01	100	3.7373E 05	0.0

Table 1 (Cont'd.)

Group No.	Upper Energy (eV)	Detector Efficiency
101	3.4733E 05	0.0
102	3.2280E 05	0.0
103	3.0000E 05	0.0
104	1.0000E 07	1.7190E-01
105	9.5000E 06	1.6610E-01
106	8.0000E 06	1.5980E-01
107	8.5000E 06	1.5400E-01
108	8.0000E 06	1.4790E-01
109	7.5000E 06	1.4340E-01
110	7.2000E 06	1.3910E-01
111	6.8000E 06	1.3490E-01
112	6.5000E 06	1.3180E-01
113	6.2000E 06	1.2870E-01
114	6.0000E 06	1.2740E-01
115	5.8000E 06	1.2660E-01
116	5.6000E 06	1.2580E-01
117	5.4000E 06	1.2480E-01
118	5.2000E 06	1.2390E-01
119	5.0000E 06	1.2270E-01
120	4.8000E 06	1.2160E-01
121	4.6000E 06	1.2000E-01
122	4.2000E 06	1.1860E-01
123	4.0000E 06	1.1770E-01
124	3.8000E 06	1.1680E-01
125	3.6000E 06	1.1580E-01
126	3.4000E 06	1.1470E-01
127	3.2000E 06	1.1340E-01
128	3.0000E 06	1.1210E-01
129	2.8000E 06	1.1080E-01
130	2.6000E 06	1.1000E-01
131	2.4000E 06	1.0890E-01
132	2.2000E 06	1.0690E-01
133	2.0000E 06	1.0400E-01
134	1.8000E 06	1.0120E-01
135	1.6000E 06	9.6200E-02
136	1.4000E 06	8.8400E-02
137	1.2000E 06	7.4600E-02
138	1.0000E 06	4.2600E-02
139	8.0000E 05	2.6000E-03
140	6.0000E 05	0.0
141	4.0000E 05	0.0

Neutron histories were started uniformly per unit lethargy from 20 MeV to the lowest energy with reported experimental data. The initial spatial coordinates of the neutrons were determined by selecting x and y uniformly over the cross-sectional area of the sample and placing z at the leading edge of the sample. Neutrons were started straight ahead in the z direction. Gamma rays produced in the sample acquired the position, time, and calculational weight of the neutrons which produced them. The calculational model for the ORNL experiment is as shown in Fig. 1.

Count rates were calculated as $\phi \times \varepsilon A$ where ϕ is the flux, ε is the detector efficiency given in Table 1, and A is the detector cross-sectional area, 19.6 cm^2. The count rates were converted to counts/MeV/ incident source neutron by multiplying by the time bin width and by dividing the count rate by the corresponding energy group width in MeV. The fraction of incident neutrons in each energy group is equal (within statistics) since the group boundaries are equally spaced in lethargy and the starting energies were selected uniformly in lethargy.

The count rates are reported as functions of the incident neutron energy. The time bins for the calculation were determined from Eq. (2).

$$T = \frac{D/C}{\sqrt{1 - \frac{1}{\left(1 + \frac{E'}{2c^2}\right)^2}}} \qquad (2)$$

where

T = flight time in sec from accelerator source to sample face for a neutron of energy E at the source,

D = distance in cm from accelerator source to sample face,

$E' = 1.91322 \times 10^{12} \times E$, where E is the energy in MeV,

c = speed of light in cm/sec.

Although included in the calculations, the flight times in the sample and to the detector are negligible compared to the time from Eq. (2). The neutron induced gamma-ray counts were removed from the published experimental results.

The calculated secondary energy spectra for the experiment included the empirically determined energy resolution of the detector given by R, the FWHM in percent

$$R = \sqrt{A + B/E}$$
$$A = 250 \text{ for neutrons, } 170 \text{ for gamma rays} \quad (3)$$
$$B = 670 \text{ for neutrons, } 288 \text{ for gamma rays}$$

and E is an energy in MeV uniformly selected in the energy group of the detected particle. The spectra were obtained by time-dependent calculations with time bins being determined by Eq. (2) where E corresponds to the energy boundaries used in compiling the experimental spectra.

IV. Comparison of Experimental and Calculated Results

The figures which follow summarize the calculation of the experimentally determined data for the two experiments. All calculations were made with the MORSE Monte Carlo code using DNA MAT 4193 MOD 2 cross-section set. The integral count rate comparisons for both neutrons and gamma rays are given in Fig. 2. In all figures the error bars represent one standard deviation of the mean value. Figures 3 through 8 give the secondary energy spectra comparisons for both neutrons and gamma rays. In the multiple energy spectra figures, each set of comparisons is plotted at the midpoint of the appropriate incident neutron energy bin (i.e., the plots at 11.25 MeV on the slanted energy scale correspond to the spectra for neutrons in the 10.0-12.5 MeV energy range incident on the sample).

V. Discussion

The count rate comparisons shown in Fig. 2 are in good general agreement. The areas of disagreement are above 10 MeV for the neutrons where the calculated count rates are too high by a few percent and from 4 to 7 MeV for the gamma rays where the calculated count rates are low by a few percent. Also, the calculated neutron count rate does not follow the structure in the experimental data between 2 and 3 MeV. A first-collision calculation indicates that about 80% of the total neutron count rate is the result of first collisions only. This effect is due to the relatively thin, 1.3 cm, sample.

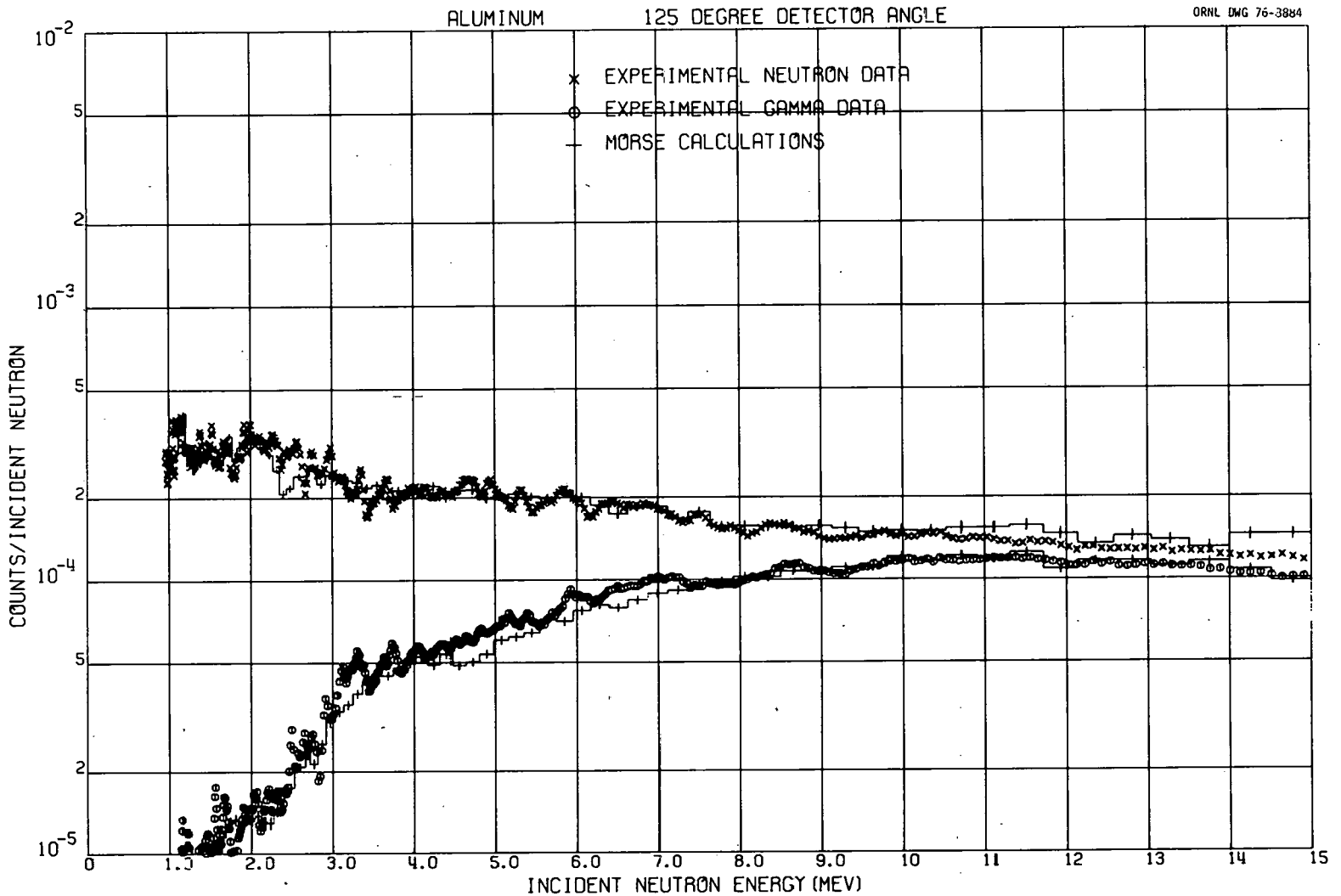

Fig. 2. Comparison of Neutron and Gamma Ray Integral Results.

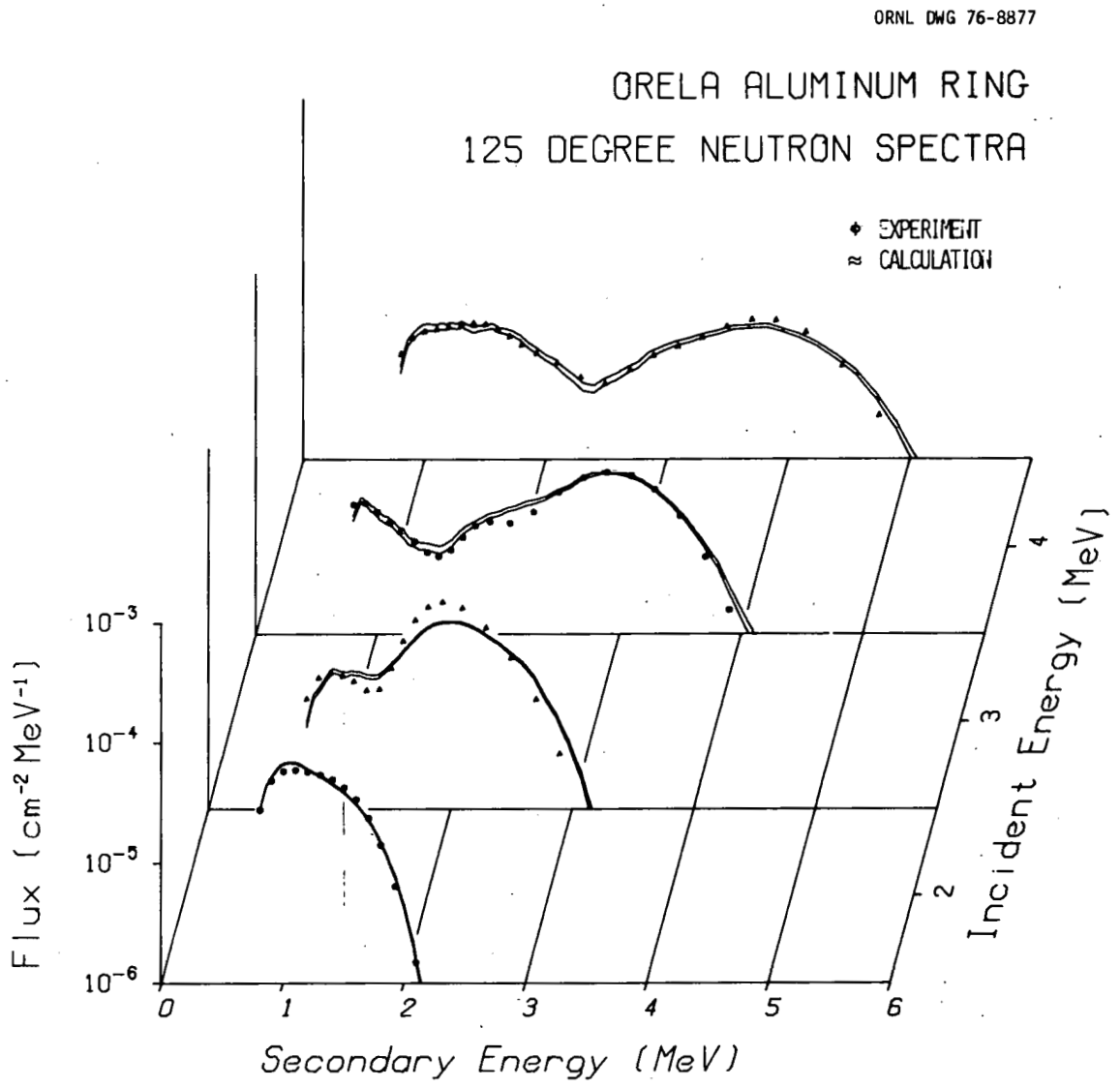

Fig. 3. Comparisons of Neutron Secondary Energy Spectra.

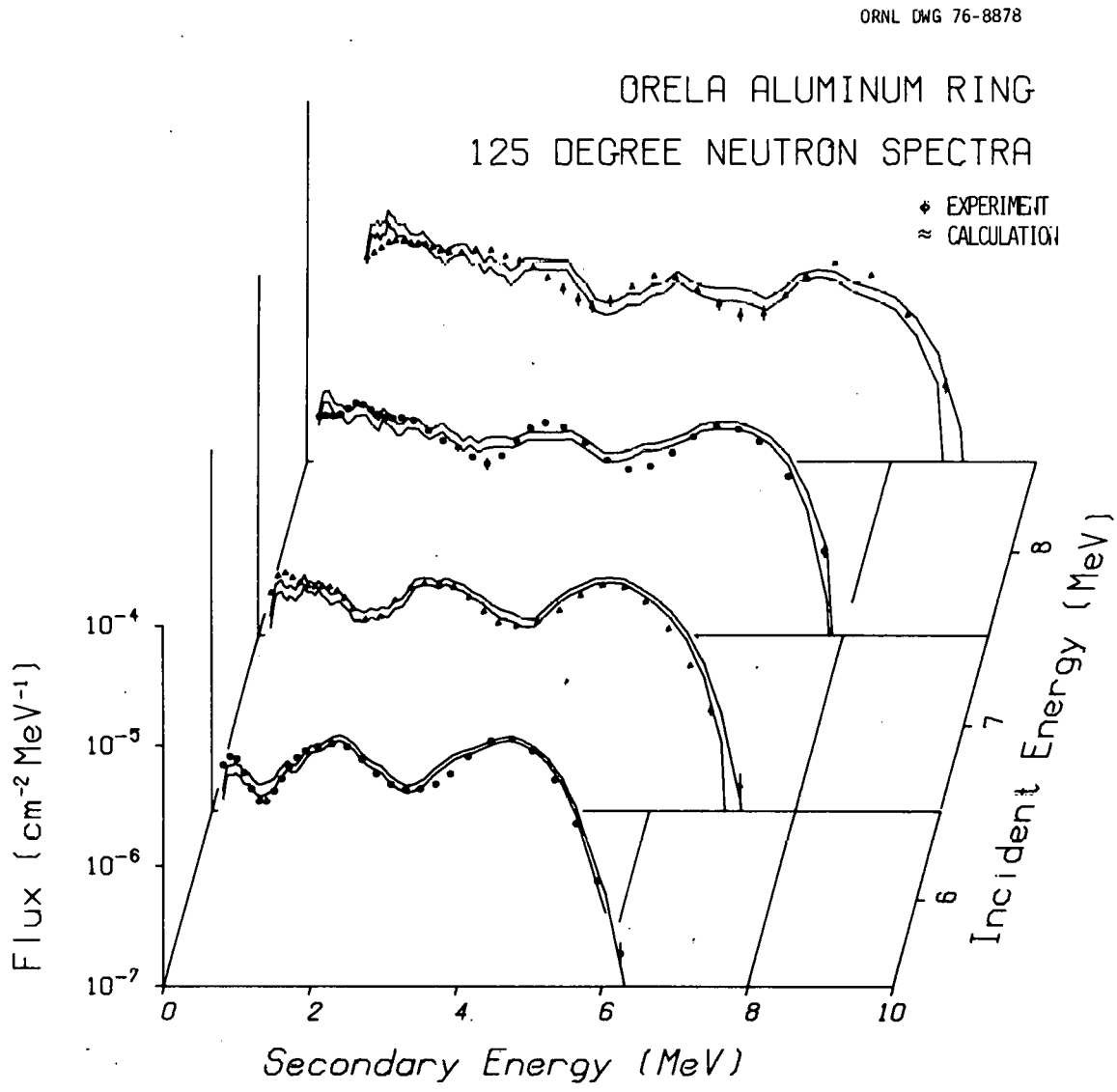

Fig. 4. Comparisons of Neutron Secondary Energy Spectra.

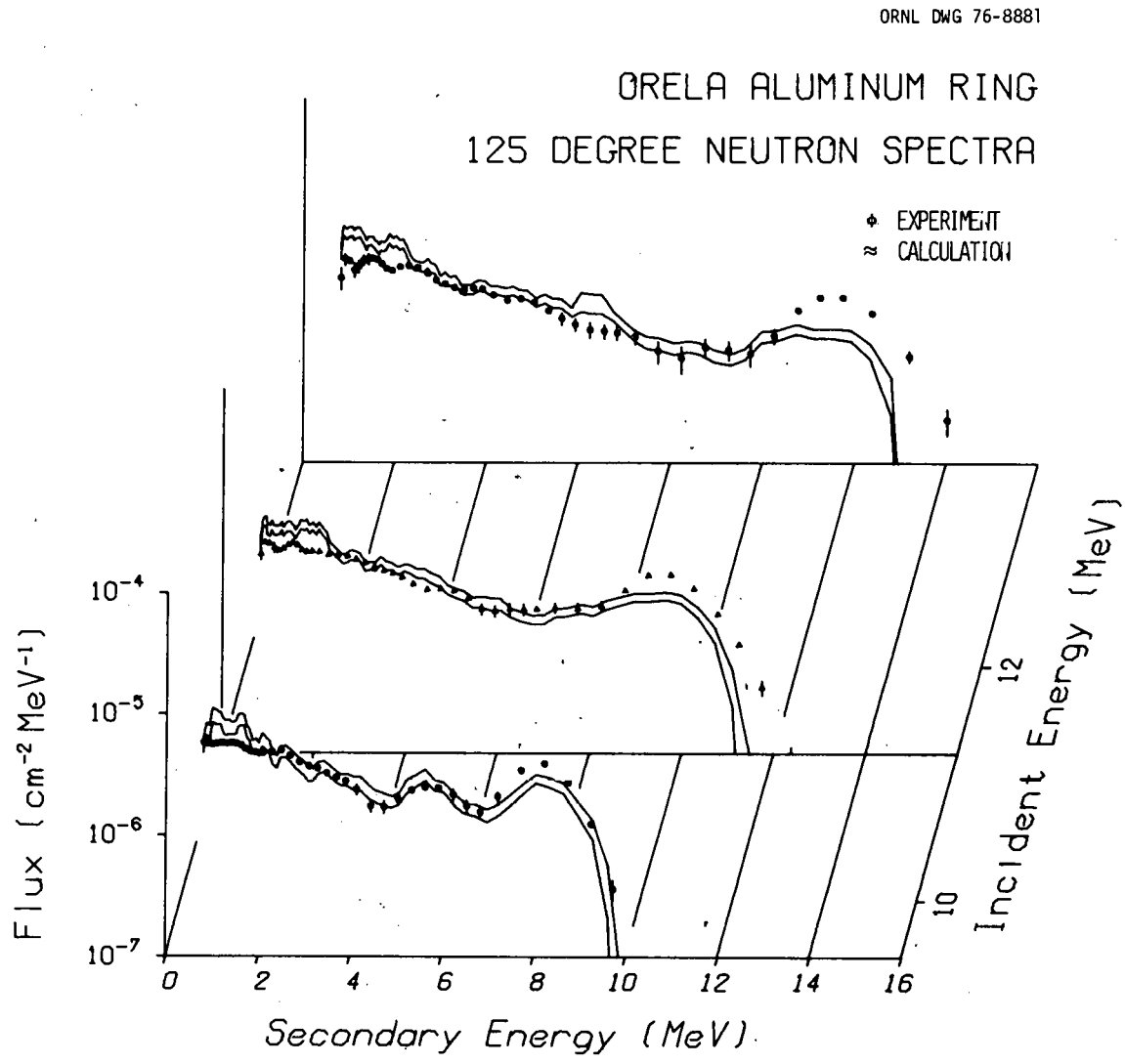

Fig. 5. Comparisons of Neutron Secondary Energy Spectra.

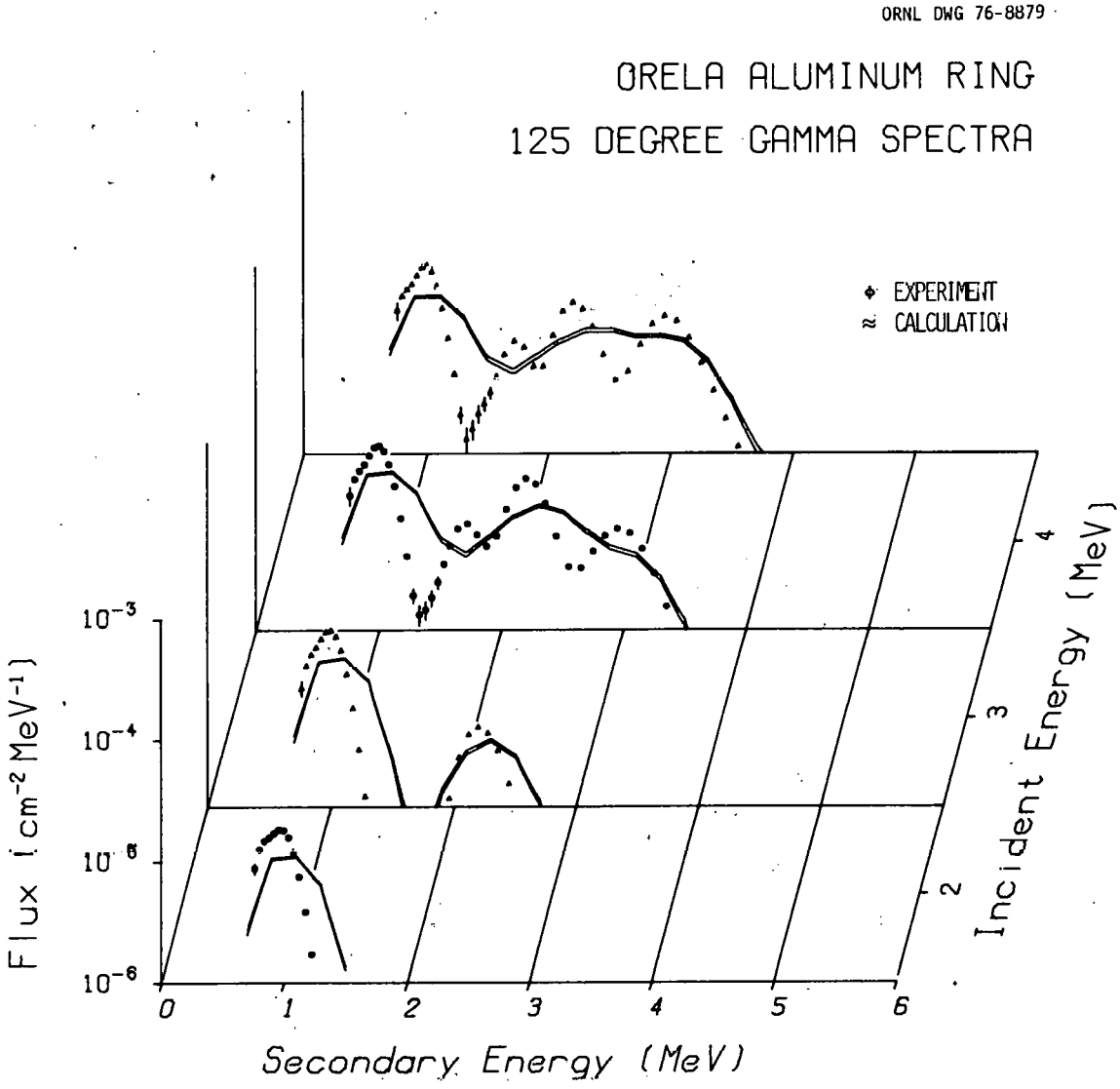

Fig. 6. Comparisons of Gamma Ray Energy Spectra.

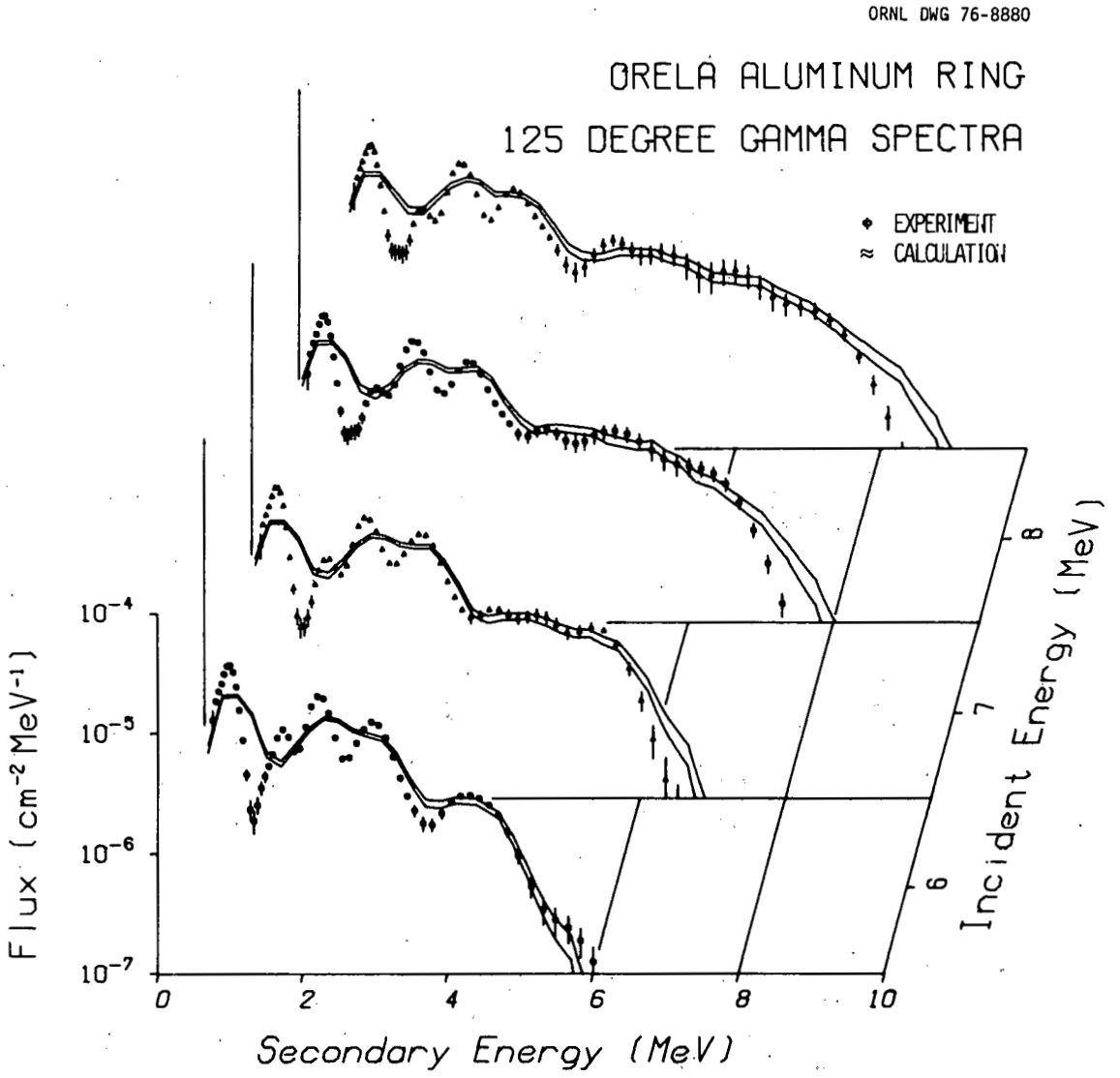

Fig. 7. Comparisons of Gamma Ray Energy Spectra.

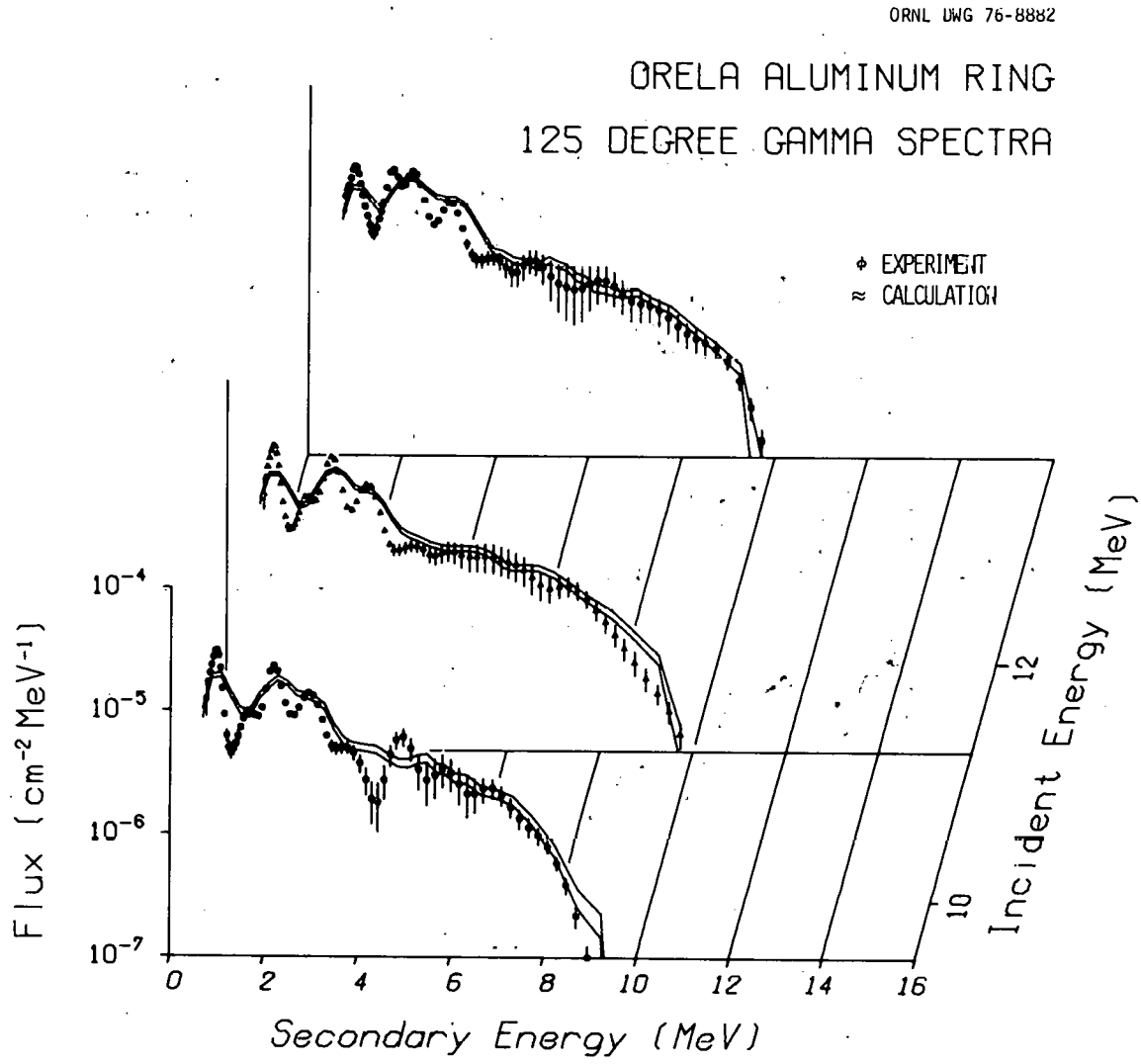

Fig. 8. Comparisons of Gamma Ray Energy Spectra.

The neutron flux spectra comparisons are shown in Figs. 3, 4, and 5. These comparisons are in good agreement, particularly for incident energies below 10 MeV. Above 10 MeV incident energy the calculated fluxes are low at high secondary energies. This effect is primarily due to the inadequacy of the P_7 Legendre expansion for elastic scattering cross section. This causes negative scattering probabilities at 125-deg. when the elastic angular distribution is highly forward peaked as it is above 10 MeV. These low calculations are reflected in the high-energy count rate and spectra calculations.

The gamma-ray flux spectra comparisons, Figs. 6, 7, and 8, show fairly good agreement about 5 MeV incident energy. Below this energy the data are questionable. The cross-section group theory itself tends to cause a smoothing effect in the calculations.

REFERENCES

1. G. L. Morgan, "Measurement of Secondary Neutrons and Gamma Rays Produced by Neutron Interactions in Aluminum Over the Incident Energy Range 1 to 20 MeV, Oak Ridge National Laboratory Report ORNL-TM-5072 (1975).

2. S. N. Cramer and E. M. Oblow, "Analyses of Neutron Scattering and Gamma-Ray Production Integral Experiments on Carbon for Neutron Energies from 1 to 15 MeV," Oak Ridge National Laboratory Report ORNL-TM-4494 (1974); see also, Nucl. Sci. Eng., 58, 33 (1975).

3. S. N. Cramer and E. M. Oblow, "Analysis of Neutron Scattering and Gamma-Ray Production Integral Experiments on Nitrogen for Neutron Energies from 1 to 15 MeV," Oak Ridge National Laboratory Report ORNL-TM-5220 (1976).

4. S. N. Cramer and E. M. Oblow, "Analysis of a Neutron Scattering and Gamma-Ray Production Integral Experiment on Oxygen for Neutron Energies from 1 to 15 MeV," Oak Ridge National Laboratory Report ORNL-TM-5535 (1976).

5. S. N. Cramer and E. M. Oblow, "Analysis of a Neutron Scattering Integral Experiment on Iron for Neutron Energies from 1 to 15 MeV," Oak Ridge National Laboratory Report ORNL-TM-

6. M. B. Emmett, "The MORSE Monte Carlo Radiation Transport Code System," Oak Ridge National Laboratory Report ORNL-4972 (1975).

7. N. M. Greene et al., "AMPX - A Modular Code System to Generate Coupled Multigroup Neutron-Gamma Cross Sections from ENDF/B," Oak Ridge National Laboratory Report ORNL-TM-3706 (1976).

Internal Distribution

1. L. S. Abbott
2. R. G. Alsmiller, Jr.
3. D. E. Bartine
4-8. S. N. Cramer
9. J. K. Dickens
10. C. Y. Fu
11. H. Goldstein (consultant)
12. D. C. Larson
13. T. A. Love
14. R. E. Maerker
15. F. C. Maienschein
16. G. L. Morgan
17-32. E. M. Oblow
33. R. W. Peelle
34. F. G. Perey
35. R. W. Roussin
36. C. R. Weisbin
37. A. Zucker
38. P. Greebler (consultant)
39. W. W. Havens, Jr. (consultant)
40. A. F. Henry (consultant)
41. R. E. Uhrig (consultant)
42-43. Central Research Library
44. ORNL Y-12 Technical Library Document Reference Section
45. Laboratory Records Department
46. Laboratory Records ORNL RC
47. ORNL Patent Office
48-49. Radiation Shielding Information Center

External Distribution

50. USERDA Oak Ridge Operations, Research & Technical Support Division, P.O. Box E, Oak Ridge, TN 37830: Director
51-77. Technical Information Center
78. Research and Technical Support Division
79-149. Given special NPD DNA distribution